

Samuel Voß*, Sylvia Saalfeld, Thomas Hoffmann, Gábor Janiga, Oliver Beuing and Philipp Berg

Fluid-structure interaction in intracranial vessel walls: The role of patient-specific wall thickness

Abstract: Computational Fluid Dynamics studies try to support physicians during therapy planning of intracranial aneurysms. However, multiple assumptions (e.g. rigid vessel walls) are required leading to a sparse acceptance of numerical approaches within the medical community.

This study incorporates multiple fluid-structural simulations for an intracranial basilar artery bifurcation. Based on the patient-specific dataset, which was acquired using optical coherence tomography, minimum, mean, maximum, and diameter-dependent thicknesses are generated and compared with respect to hemodynamic and wall stress parameters.

The comparison of different wall thickness models revealed a strong variability among the analyzed parameters depending on the corresponding assumption. Using the patient-specific configuration as a reference, constant thicknesses lead to differences of up to 100 % in the mean wall stresses. Even the diameter-dependent thickness results in deviations of 32 %, demonstrating the wide variability of computational predictions due to inaccurate assumptions.

The findings of this study highlight the importance of geometry reconstruction including accurate wall thickness reproduction for fluid-structure simulations. Patient-specific wall thickness seems to be out of alternatives regarding the prediction of wall stress distributions.

Keywords: Fluid-structure interaction, Computational Fluid Dynamics, cerebral aneurysm, wall thickness.

<https://doi.org/10.1515/cdbme-2018-XXXX>

1 Introduction

Computational Fluid Dynamics (CFD) is a widely used tool to understand aneurysm progression and rupture mechanisms [1-3]. However, several assumptions are still common due to limited measurement accuracies as well as capabilities and computational resources. Especially the consideration of rigid vessel walls is used in almost all computational studies dealing with intracranial hemodynamics. However, minor wall movements due to the pulsatile flow character were reported [4,5] and - most importantly - differences in the local vessel wall thickness are frequently observed [6].

In 2009, Bazilevs et al. [7] proposed a simple approach to construct variable vessel wall thicknesses. They concluded that the assumption of rigid vessel walls leads to a significant overestimation of relevant hemodynamic parameters such as wall shear stress (WSS). Cebal et al. [8] found a correlation between the wall thickness as well as its stiffness and the rupture site. An extensive study regarding fluid-structure-interaction (FSI) computations for intracranial aneurysms was carried out by Valencia et al. [9]. They analysed a patient-specific saccular aneurysm using 13 different simulation setups and suggested using one-directional FSI with a hyperelastic material model. However, still no real local wall thicknesses were included in their investigation. Voß et al. [10] compared constant and patient-specific wall thickness with regard to the aneurysm rupture site using FSI. The results highlight the importance of accurate wall thickness description.

The present study considers patient-specific wall thickness and aims to compare different artificial wall generation approaches to evaluate their necessity for blood flow and wall stress prediction in a basilar artery bifurcation. Hence, FSI simulations are compared to evaluate the necessity of local wall thicknesses within hemodynamic computations. In this regard, the minimum, mean, maximum, and diameter-dependent values of the patient-specific thickness were used for generating the arterial vessel wall.

*Corresponding author: Samuel Voß: University of Magdeburg, Universitätsplatz 2, 39106 Magdeburg, Germany, e-mail: samuel.voss@ovgu.de

Thomas Hoffmann, Sylvia Saalfeld: Research campus STIMULATE, University of Magdeburg, Magdeburg, Germany

Oliver Beuing: Institute of Neuroradiology, University Hospital Magdeburg, Magdeburg, Germany

Gábor Janiga, Philipp Berg: Research campus STIMULATE, University of Magdeburg, Magdeburg, Germany

2 Materials and Methods

2.1 Case description / image acquisition

A complete Circle of Willis and adjacent vessels were harvested from a 36-year-old male person post mortem and further investigated with the approval of the local ethics committee (see Figure 1). Intravascular optical coherence tomography (OCT) of the vessel walls was performed with the Terumo Lunawave system (Terumo Corporation, Tokyo, Japan), which includes an OCT catheter (Fastview, Terumo Corporation, Tokyo, Japan) with a distal diameter of 2.6 F. The axial spatial resolution is below $20\ \mu\text{m}$ with good soft tissue contrast and real-time visualization (158 fps). A slice thickness of $127\ \mu\text{m}$ was reached with a radial resolution of $13\ \mu\text{m}$ [11].

2.2 Vascular reconstruction

The manual segmentation was conducted using MeVisLab 2.6.2 (MeVis Medical Solutions AG, Bremen, Germany). Afterwards, the vessels were virtually inflated (see Figure 2, top) [12]. Small artefacts (e.g. small bumps of the mesh due to noise of the OCT data) were manually corrected and the mesh quality was further improved using Sculpttris 1.02 (Pixologic, Los Angeles, USA). Finally, the data sets of both OCT scans were combined to model the bifurcation. Before, the position of the bifurcation was manually marked in the OCT data sets. At this bifurcation, local smoothing was carried out in Sculpttris. The segmentation result is displayed in Figure 2d and is evaluated by an experienced neuroradiologist.

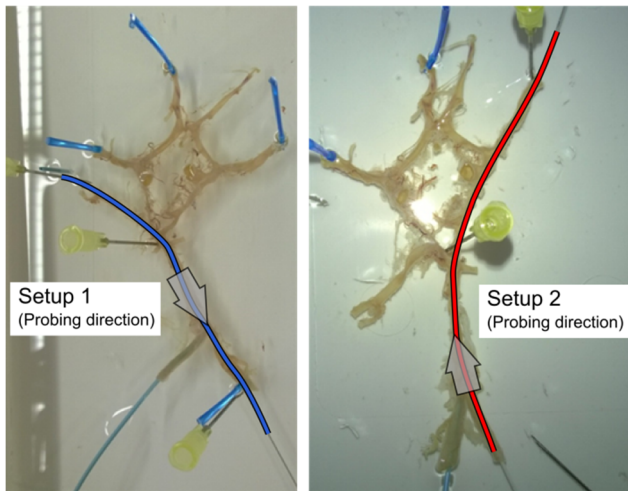


Figure 1: Depiction of both OCT imaging setups (arrows indicate the direction of probing).

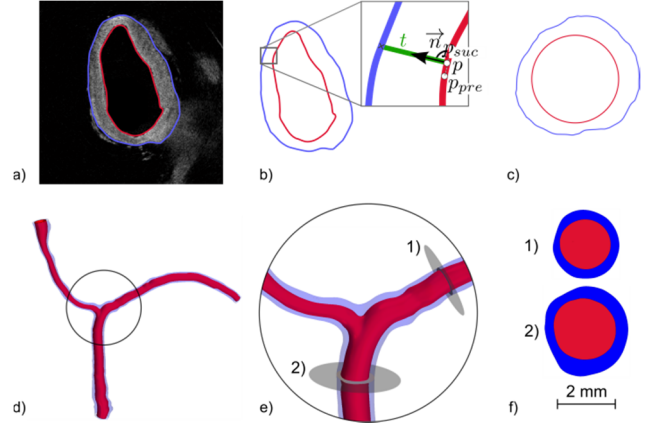


Figure 2: Virtual inflation of vessel wall contours. In a), the OCT slice with the inner vessel wall (red) and the outer vessel wall (blue) is depicted. In b), the wall thickness t is determined by extracting the normal vector for each inner wall contour point p and its intersection point with the outer wall. In c), the virtually inflated, i.e., circular, inner vessel wall is depicted, where for each point the wall thickness is transferred. The reconstructed geometry is shown in d), while in e) and f), the location of the minimum and maximum local wall thickness and its cross-sectional view is illustrated.

2.3 Hemodynamic simulation

Hemodynamic FSI simulations were carried out for five configurations based on the segmented surface: constant minimum (0.2 mm), mean (0.4 mm), maximum (0.6 mm), diameter dependent (22 % of local diameter), and patient-specific wall thickness (based on OCT measurement), which serves as a reference, respectively.

The models were spatially discretized using Star-CCM+ V9.04 (Siemens Product Lifecycle Management Software Inc., Plano, TX, USA 75024) resulting in 1.2 to 1.6 million cells depending on the wall thickness. The same software was used for the FSI computations, applying the following boundary conditions: 1) A steady-state velocity value derived from a cycle-averaged 7T phase-contrast magnetic resonance imaging measurement [13] was applied at the inlet, 2) A zero pressure condition was defined at both outlets, 3) A two-way coupling was carried out at the interface between the fluid and solid domain.

The fluid was assumed to be non-Newtonian (Carreau-Yasuda) and incompressible ($\rho_f = 1055\ \text{kg/m}^3$). For the vessel wall, homogenous and isotropic material properties were defined (Young's modulus = 1 MPa, Poisson ratio = 0.45, $\rho_s = 1050\ \text{kg/m}^3$).

3 Results

To compare the different concepts of wall thickness generation, the simulations were performed using equivalent conditions except for the variation of the arterial geometry. Starting with a qualitative comparison, Figure 3 shows the equivalent stress on the inner (top) and outer (bottom) surface depending on the wall thickness. For minimum wall thickness, disproportional values are indicated while in other cases the changes remain smaller. The maximum equivalent stress inside the artery ranges from 84 to 216 kPa based on maximum and minimum wall thickness, respectively.

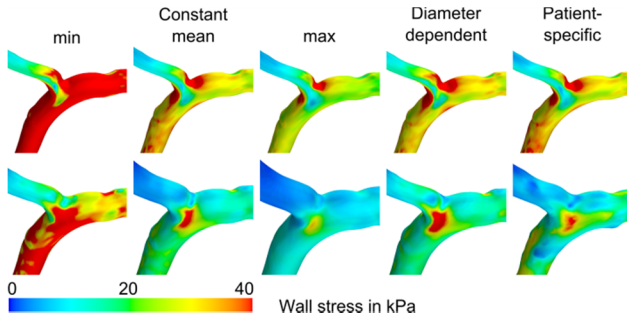


Figure 3: Qualitative simulation results based on the different wall thickness approaches showing equivalent stress of the inner (top row) and outer surface (bottom row).

To support the qualitative findings, a quantitative comparison is addressed regarding 1) the different wall thickness configurations and 2) case internal variations of the local equivalent stresses along the vessel subdomains, see Figure 4. Accordingly, the stress level varies highly in both cases. The results of the bifurcation (subdomain B) itself, representing a potential region for aneurysm growth, are

similar to those of the region proximal (Ax: basilar artery) and distal (Cx: right posterior cerebral artery, PCA). The left PCA (Dx) shows much lower stress values than the right PCA. Comparing the patient-specific configuration, the stresses fluctuate approximately around 20 kPa, except for the left distal vessel section of the PCA (e.g., values less than 8 kPa).

Overall, only small changes in the hemodynamics are found. Maximum deviation of flow velocity and WSS is 2.3 % and approximately 10 %, respectively. In contrast, the results of the solid domain are much more diverse. Extreme deviations of the minimum thickness case with partly more than 100 % are visible; others remain below 17 % (mean), 38 % (max), and 32 % (diameter dependent), respectively.

4 Discussion and Conclusions

Analysing the differences caused by varying wall thickness approaches, it must be noted that the changes in the hemodynamic solutions are very small compared to the results inside the arterial wall. However, these changes might be relevant for CFD issues and the decision, whether FSI is needed for a proper flow prediction. About 10 % higher WSS might yield a big difference and an aneurysmal geometry could even intensify this increase.

Based on the presented findings, the variation of minimum and maximum wall thickness is too high to represent a reasonable simplification. Especially a very small wall thickness is sensitive to overestimation of wall stresses. The implementation of a mean or diameter-dependent wall thickness is widely used. Nevertheless, as shown in the results, variations of 16.7 % (mean) and 31.2 % (diameter

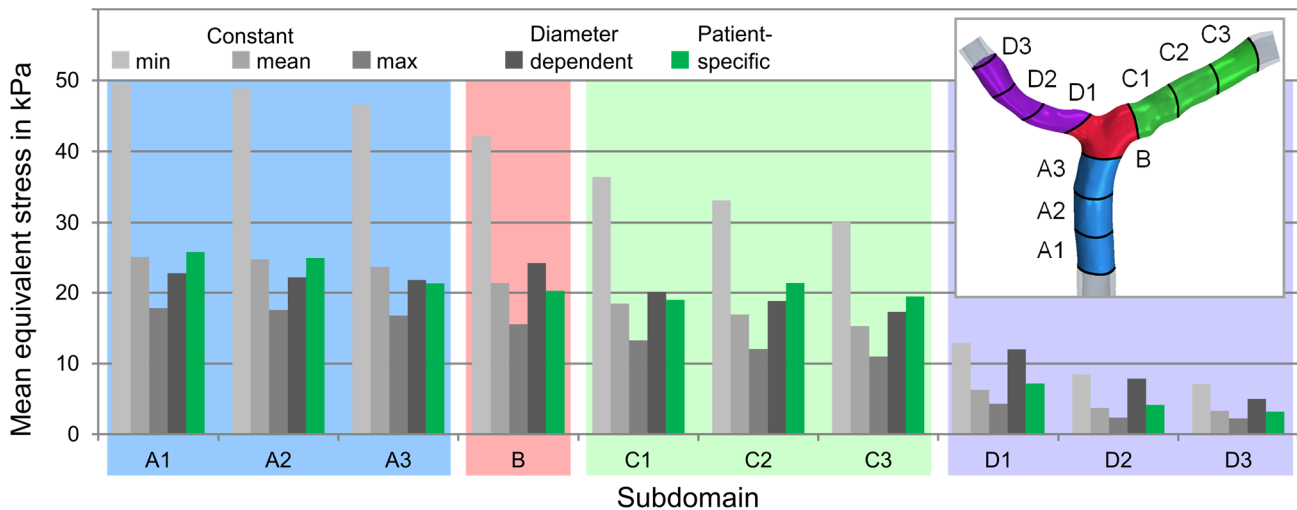


Figure 4: Mean equivalent stress depending on 1) the wall thickness generation approach and 2) the subdomain.

dependent) to the patient-specific stresses can still occur.

However, the results of the patient-specific configuration are not seen as ground truth - uncertainty and simplifications are still present. For this reason, the focus is on relative quantities instead of absolute values, since the conditions are equivalent within all simulations.

Firstly, some limitations concern the imaging, thus it must be pointed out that the vessel position and arrangement as well as the fixation differ from the in vivo setting. The resolution of image acquisition is limited. However, OCT represents the best available intravascular measurement technique.

Secondly, the geometry reconstruction was carried out using an in-house inflating technique [12]. This ensures a realistic reproduction of the vessel anatomy, but minor deviations cannot be ruled out completely. Also, a local smoothing is required to provide appropriate vessel surfaces. Nevertheless, all modifications were compared to the initial data sets to guarantee no falsification.

Thirdly, due to the lack of patient-specific data on flow and vessel wall properties, all values for the flow inlet and material model are taken from a representative 7T PC-MRI measurement and the literature, respectively. However, differences are present depending on the specific patient, age, activity, location, biological constitution, etc. Especially the assumption of an isotropic, homogenous, linear-elastic material represents a simplification aiming on achievable simulation complexity. Nevertheless, since material information outside of the arteries are unknown and the deformations throughout the cardiac cycle are rather small, the assumption of a free deformation is valid.

In conclusion, the findings of this study highlight the importance of geometry reconstruction including the accurate wall thickness reproduction for fluid-structure simulations. For the prediction of wall stress distributions, the use of patient-specific wall thickness seems to be out of alternatives. Therefore, future models should contain more complex material models and the investigations require an extension to aneurysms with known local wall thickness.

Author Statement

Research funding: This work was partly funded by the Federal Ministry of Education and Research in Germany within the Research Campus *STIMULATE* under grant number 13GW0095A.

Conflict of interest: Authors state no conflict of interest.

Informed consent: Informed consent has been obtained from all individuals included in this study.

Ethical approval: The research related to human use complies with all the relevant national regulations, institutional

policies and was performed in accordance with the tenets of the Helsinki Declaration, and has been approved by the authors' institutional review board or equivalent committee.

References

- [1] Cebal JR, Mut F, Sforza D et al. Clinical application of image-based CFD for cerebral aneurysms. *Int J Numer Method Biomed Eng* 2011;27:977–992.
- [2] Chung B, Cebal JR. CFD for evaluation and treatment planning of aneurysms: Review of proposed clinical uses and their challenges. *Ann Biomed Eng* 2015;43:122–138.
- [3] Janiga G, Berg P, Sugiyama S et al. The computational fluid dynamics rupture challenge 2013–phase I: Prediction of rupture status in intracranial aneurysms. *Am J Neuroradiol* 2015;36:530–536.
- [4] Hayakawa M, Katada K, Anno H et al. CT angiography with electrocardiographically gated reconstruction for visualizing pulsation of intracranial aneurysms: Identification of aneurysmal protuberance presumably associated with wall thinning. *Am J Neuroradiol* 2005;26:1366–1369.
- [5] Hayakawa M, Maeda S, Sadato A et al. Detection of pulsation in ruptured and unruptured cerebral aneurysms by electrocardiographically gated 3-dimensional computed tomographic angiography with a 320-row area detector computed tomography and evaluation of its clinical usefulness. *Neurosurg* 2011;69:843–851.
- [6] Song J, Park JE, Kim HR, Shin YS. Observation of cerebral aneurysm wall thickness using intraoperative microscopy: Clinical and morphological analysis of translucent aneurysm. *Neurol Sci* 2015;36:907–912.
- [7] Bazilevs Y, Hsu M, Benson DJ et al. Computational fluid–structure interaction: Methods and application to a total cavopulmonary connection. *Comp Mech* 2009;45:77–89.
- [8] Cebal JR, Vazquez M, Sforza DM et al. Analysis of hemodynamics and wall mechanics at sites of cerebral aneurysm rupture. *J Neurointerv Surg* 2015;7:530–536.
- [9] Valencia A, Burdiles P, Ignat M, et al. Fluid structural analysis of human cerebral aneurysm using their own wall mechanical properties. *Comp Math Meth Med* 2013;1–18.
- [10] Voß S, Glaßer S, Hoffmann T et al.: Fluid-structure simulations of a ruptured intracranial aneurysm: Constant versus patient-specific wall thickness. *Comput Math Meth Med* 2016;1–8
- [11] Hoffmann T, Glaßer S, Boese A et al. Experimental investigation of intravascular OCT for imaging of intracranial aneurysms. *Int J Comput Assist Radiol Surg* 2016;11:231–41.
- [12] Glaßer S, Hoffmann T, Boese A et al. Histology-based evaluation of optical coherence tomographic characteristics of the cerebral artery wall via virtual inflating. *Eurographics Workshop on Visual Computing for Biology and Medicine* 2015:149–158.
- [13] Berg P, Stucht D, Janiga G et al. Cerebral blood flow in a healthy circle of Willis and two intracranial aneurysms: Computational fluid dynamics versus four-dimensional phase-contrast magnetic resonance imaging. *J Biomech Eng* 2014;136:1–9